Journal of Sound and Vibration (2002) **254**(4), 787–800
doi:10.1006/jsvi.2001.4124, available online at http://www.idealibrary.com on IDEAL®

A NEW METHOD FOR IN-PLANE VIBRATION ANALYSIS OF CIRCULAR RINGS WITH WIDELY DISTRIBUTED DEVIATION

Y. J. YOON AND J. M. LEE

School of Mechanical and Aerospace Engineering, Seoul National University, San 56-1, *Shillim-dong, Kwanak-gu, Seoul* 151-742, *Korea. E-mail: leejm@gong.snu.ac.kr*

S. W. YOO

ArvinMeritor Technical Center, 950 *W* 450 *S*, *Columbus*, *IN* 47201, *U.S.A. E-mail: sung-woo.yoo@arvinmeritor.com*

AND

H. G. CHOI

Turbo and Power Machinery Research Center, Seoul National University, San 56-1, *Shillim-dong, Kwanak-gu, Seoul* 151-742, *Korea. E-mail: hgchoi@vib.snu.ac.kr*

(*Received* 25 *June* 2001, *and in final form* 3 *December* 2001)

A new analytical method was developed to predict the in-plane mode shapes and the natural frequencies of a ring with widely distributed deviation. The Laplace transform was used to find the exact solution of eigenvalue problem without assuming any trial functions and finite elements. The widely distributed deviation was effectively formulated in the theory using Gauss–Legendre quadrature. The validity of the proposed method was examined through finite element analysis and modal test. The effects of partial change of the density, the stiffness, and the thickness on the natural frequencies of the ring were investigated.

1. INTRODUCTION

In the past few years, structures of asymmetric ring shape have been investigated to analyze related structures widely used in industries. The asymmetry of a ring-type structure is normally due to partial cuts, added masses, non-uniform geometry, different material properties, etc., and the natural frequencies and mode shapes of these structures are changed depending on the amount of asymmetry.

Many methods have been proposed for the analysis of rings with various asymmetries. Allaei, Soedel and Young investigated the free vibration behavior of rings with attached ground spring, attached torsional spring, and a point mass, using the receptance method [1, 2]. Cerep used a harmonic approximation for the deflection function of a ring and Lagrange equation to analyze the in-plane vibration of circular rings on a tensionless foundation [3]. Rossi investigated the effect of non-uniform cross-section to the in-plane vibration of circular rings [4]. He used the finite element method in which explicit expressions for the stiffness and mass matrices were derived for generic elements of ring's circular central axis.

0022-460X/02/$35.00

To find an exact solution to the analysis of circular rings with small local deviation not using the approximate method or the finite element method, Hong and Lee developed a new method that find the natural frequencies and mode shapes simultaneously without any trial functions for mode shapes and the use of finite elements [5]. They used the Laplace transformation method for the eigenvalue analysis, and investigated the effect of a small local deviation on the natural frequencies and mode shapes of a circular ring.

Recently, Gutierrez and Laura [6] proposed a method for the analysis of a non-uniform ring using the differential quadrature method, while Wake *et al.* [7] investigated the separation of natural frequencies of a cracked ring using a simple energy-based model. Hwang, Fox and William obtained the natural frequencies and the mode shapes of thin rings with in-plane profile variations [8, 9]. They used Fourier series to describe the inner and outer ring surfaces and analyzed the in-plane vibration characteristics by means of the Rayleigh–Ritz method.

Chung and Lee [10] developed a new conical ring element used in connection with FEM in order to consider the effects of slight local deviations from an axisymmetric ring, and analyzed the free vibrations of a nearly axisymmetric shell structure such as a Korean bell, using this element. Kim *et al.* [11] analyzed the beating response of a ring-stiffened cylindrical shell with an attached concentrated mass, which is a simplified model of a Korean bell on the basis of the receptance method. They showed the effects of the ring stiffening and the asymmetry due to the concentration mass on the beating response.

In this study, an analysis method was developed for the eigenvalue analysis of circular rings that have cross-sectional deviation over large circumferential length, using the Laplace transformation and Gauss quadrature. The Gauss quadrature is introduced to analyze the effect of this widely distributed circumferential asymmetry, because the method of Hong and Lee is suitable only for a deviation of a short circumferential length. The natural frequencies and mode shapes of rings with various asymmetries were calculated and compared with the results from FEM and modal test to examine the validity of this analysis. Based on the verified results, several simulations were performed to investigate the characteristics of the natural frequencies.

2. THEORY

2.1. EQUATION OF MOTION

If the thickness of a ring is thin compared with the radius, the effect of shear force and rotational inertia can be neglected and the equation of motion for in-plane vibration of a circular ring is

$$\frac{\partial^3 M_b}{\partial\theta^3} + \frac{\partial M_b}{\partial\theta} = R^2\frac{\partial^2}{\partial t^2}\left[mv - \frac{\partial}{\partial\theta}(mu)\right], \qquad M_b = \frac{EI}{R^2}\left(\frac{\partial^2 u}{\partial\theta^2} + \frac{\partial v}{\partial\theta}\right), \tag{1}$$

where M_b, u, v, m and R are the bending moment, radial displacement, circumferential displacement, mass per unit length, and radius of a circular ring respectively [12, 13].

For a ring that has a circumferential deviation widely distributed over $\Delta\theta$ as shown in Figure 1, the Heaviside unit step function can be used to express the properties in the circumferential direction. Therefore, stiffness and mass per unit length of the ring can be represented as

$$\begin{aligned} EI &= (EI)_u + (EI)_a[\mathrm{H}(\theta - \theta_{\mathrm{I}}) - \mathrm{H}(\theta - \theta_{\mathrm{II}})], \\ m &= m_u + m_a[\mathrm{H}(\theta - \theta_{\mathrm{I}}) - \mathrm{H}(\theta - \theta_{\mathrm{II}})], \end{aligned} \tag{2}$$

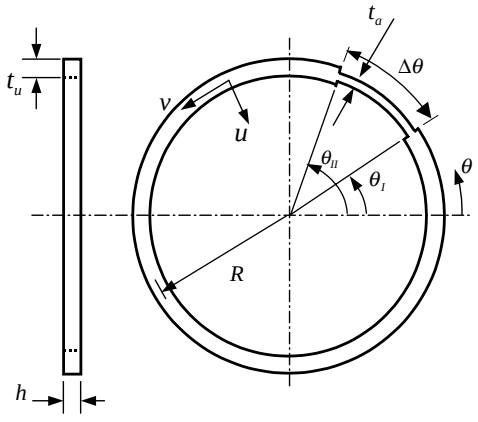

Figure 1. Circular ring with widely distributed deviation.

where H is the Heaviside unit step function, and the subscripts u and a denote original ring's properties and added properties respectively.

Assuming no circumferential strain in the neutral axis of the ring and $v(\theta, t) = V(\theta)e^{j\omega t}$, we can derive the eigenvalue problem from equations (1) and (2) [5]. The eigenvalue problem is represented as

$$[V^{(6)} + 2V^{(4)} + V'' - \lambda(V'' - V)] - G_m + G_{EI} = 0, \tag{3}$$

where

$$G_m = \lambda \frac{m_a}{m_u} [(V'' - V)(\mathrm{H_I} - \mathrm{H_{II}}) + V'(\delta_\mathrm{I} - \delta_\mathrm{II})],$$

$$G_{EI} = \frac{(EI)_a}{(EI)_u} [(V^{(6)} + 2V^{(4)} + V'')(\mathrm{H_I} - \mathrm{H_{II}}) + (3V^{(5)} + 4V''' + V')(\delta_\mathrm{I} - \delta_\mathrm{II}) + 3(V^{(4)} + V'')(\delta'_\mathrm{I} - \delta'_\mathrm{II}) + (V''' + V')(\delta''_\mathrm{I} - \delta''_\mathrm{II})].$$

In equation (3), the primes denote derivatives with respect to θ, and λ, $\mathrm{H_I}$, $\mathrm{H_{II}}$, δ_I, and δ_II are defined as

$$\lambda = \frac{m_u R^4 \omega^2}{(EI)_u}, \quad H_\mathrm{I} = \mathrm{H}(\theta - \theta_\mathrm{I}), \quad H_\mathrm{II} = \mathrm{H}(\theta - \theta_\mathrm{II}),$$
$$\delta_\mathrm{I} = \delta(\theta - \theta_\mathrm{I}), \quad \delta_\mathrm{II} = \delta(\theta - \theta_\mathrm{II}). \tag{4}$$

To solve the eigenvalue problem, the Laplace transformation is applied to equation (3):

$$[s^6 + 2s^4 + (1 - \lambda)s^2 - \lambda]\bar{V}(s) = [s^5 + 2s^3 + (1 - \lambda)s]V(0) + (s^4 + 2s^2 + 1 - \lambda)V'(0) + (s^3 + 2s)V''(0) + (s^2 + 2)V'''(0) + sV^{(4)}(0) + V^{(5)}(0) - \mathscr{L}(G_m) + \mathscr{L}(G_{EI}), \tag{5}$$

where

$$\mathscr{L}(G_m) = \lambda \frac{m_a}{m_u} \int_{\theta_\mathrm{I}^+}^{\theta_\mathrm{II}^-} e^{-s\theta}\{sV'(\theta) - V(\theta)\}\,\mathrm{d}\theta,$$

$$\mathscr{L}(G_{EI}) = \frac{(EI)_a}{(EI)_u}(s^3 + s) \int_{\theta_\mathrm{I}^+}^{\theta_\mathrm{II}^-} e^{-s\theta}\{V'''(\theta) + V'(\theta)\}\,\mathrm{d}\theta.$$

The integration can be normally performed using Gauss quadrature, but the integration in equation (5) cannot be directly performed, because θ_{I}^{+} and θ_{II}^{-} cannot be used in the Gauss quadrature integration. Therefore, continuity conditions at θ_{I} and θ_{II} are used to perform the integration by Gauss quadrature.

2.2. GAUSS QUADRATURE AND CONTINUITY CONDITIONS

For the Laplace transform of G_m and G_{EI}, the continuity conditions at θ_{I} and θ_{II} should be considered because the start and the end points of the integral are on the geometrically discontinuous points. The continuity conditions at θ_I are

$$V(\theta_{\mathrm{I}}^{+}) = V(\theta_{\mathrm{I}}^{-}), \quad V'(\theta_{\mathrm{I}}^{+}) = V'(\theta_{\mathrm{I}}^{-}), \tag{6a}$$

$$V'''(\theta_{\mathrm{I}}^{+}) + V'(\theta_{\mathrm{I}}^{+}) = \frac{(EI)_u}{(EI)_u + (EI)_a}[V'''(\theta_{\mathrm{I}}^{-}) + V'(\theta_{\mathrm{I}}^{-})] \tag{6b}$$

and the continuity conditions at θ_{II} are analogous [5].

The continuity conditions of a ring with a local deviation can be easily considered, because the integration can be simply performed assuming a simple function in the small range of integration and the continuity conditions are used after the integration. We used the Gauss quadrature for the integration of the ring with widely distributed deviation. However, the integration cannot be performed before the continuity condition is considered, because θ_{I}^{+} and θ_{II}^{-} cannot be directly used in the Gauss quadrature integration.

To consider the continuity conditions before the integration, the range of the integration is changed by a coordinate transformation equation

$$y = \frac{2\theta - (\theta_{\mathrm{I}}^{+} + \theta_{\mathrm{II}}^{-})}{\theta_{\mathrm{II}}^{-} - \theta_{\mathrm{I}}^{+}}. \tag{7}$$

Using this transformation equation, the integrals in equation (5) are changed to the following equation:

$$\mathscr{L}(G_m) = \lambda \frac{m_a}{m_u} \int_{-1}^{1} \mathrm{e}^{-sy_{IN}} \{sV'(y_{IN}) - V(y_{IN})\} \, \mathrm{d}y, \tag{8a}$$

$$\mathscr{L}(G_{EI}) = \frac{(EI)_a}{(EI)_u}(s^3 + s) \int_{-1}^{1} \mathrm{e}^{-sy_{IN}} \{V'''(y_{IN}) + V'(y_{IN})\} \, \mathrm{d}y, \tag{8b}$$

where $y_{IN} = \frac{1}{2}\{(\theta_{\mathrm{II}}^{-} - \theta_{\mathrm{I}}^{+})y + (\theta_{\mathrm{I}}^{+} + \theta_{\mathrm{II}}^{-})\}$. The integrands of the above equation have constants θ_{I}^{+} and θ_{II}^{-}, and these constants are changed to θ_{I}^{-} and θ_{II}^{+} by applying the continuity conditions (6) when y is –1 and 1. Then, we can obtain the equation

$$\mathscr{L}(G_m) = \lambda \frac{m_a}{m_u} \int_{-1}^{1} \mathrm{e}^{-sy_{OUT}} \{sV'(y_{OUT}) - V(y_{OUT})\} \, \mathrm{d}y, \tag{9a}$$

$$\mathscr{L}(G_{EI}) = \frac{(EI)_a}{(EI)_u + (EI)_a}(s^3 + s) \int_{-1}^{1} \mathrm{e}^{-sy_{OUT}} \{V'''(y_{OUT}) + V'(y_{OUT})\} \, \mathrm{d}y, \tag{9b}$$

where $y_{OUT} = \frac{1}{2}\{(\theta_{\mathrm{II}}^{+} - \theta_{\mathrm{I}}^{-})y + (\theta_{\mathrm{I}}^{-} + \theta_{\mathrm{II}}^{+})\}$.

Applying the Gauss–Legendre quadrature, the final forms of the integrations are

$$\mathscr{L}(G_m) = \lambda \frac{m_a}{m_u} \frac{\Delta\theta}{2} \sum_{i=1}^{N} w_i e^{-s\theta_i}(sV_i' - V_i), \tag{10a}$$

$$\mathscr{L}(G_{EI}) = \frac{(EI)_a}{(EI)_u + (EI)_a} \frac{\Delta\theta}{2} \sum_{i=1}^{N} w_i e^{-s\theta_i}(s^3 + s)(V_i''' + V_i'), \tag{10b}$$

where i denotes the Gaussian point from 1 to N and w_i denotes the weighting coefficient at the ith Gaussian point.

2.3. ANALYSIS FOR THE MODE SHAPE AND NATURAL FREQUENCY

The inverse Laplace transform of equations (5) and (10) can be represented by the Bromwich integral, and can be finally obtained by using the Residue theorem [14]. Assuming that $e^{s\theta}\bar{V}(s)$ has simple poles at $s = \pm Z_1, \pm Z_2, \pm Z_3$, we can show that

$$\begin{aligned} V(\theta) = &\sum_{j=1}^{3} [A_j \cosh(Z_j\theta) + B_j \sinh(Z_j\theta)] \\ &+ \sum_{i=1}^{N} \sum_{j=1}^{3} \mathrm{H}(\theta - \theta_i)[C_{ij} \cosh\{Z_j(\theta - \theta_i)\} + D_{ij} \sinh\{Z_j(\theta - \theta_i)\}], \end{aligned} \tag{11}$$

where

$$\begin{aligned} A_j &= \frac{1}{Q_j}[\{Z_j^5 + 2Z_j^3 + (1-\lambda)Z_j\}V(0) + (Z_j^3 + 2Z_j)V''(0) + Z_j V^{(4)}(0)], \\ B_j &= \frac{1}{Q_j}[(Z_j^4 + 2Z_j^2 + 1 - \lambda)V'(0) + (Z_j^2 + 2)V'''(0) + V^{(5)}(0)], \\ C_{ij} &= \frac{Z_j}{Q_j}\lambda M^* w_i V'(\theta_i) - \frac{Z_j^3 + Z_j}{Q_j}(EI)^* w_i[V'''(\theta_i) + V'(\theta_i)], \\ D_{ij} &= -\frac{1}{Q_j}\lambda M^* w_i V(\theta_i), \quad Q_j = 3Z_j^5 + 4Z_j^3 + (1-\lambda)Z_j, \ j = 1,2,3 \\ M^* &= \frac{m_a}{m_u}\frac{\Delta\theta}{2}, \qquad (EI)^* = \frac{(EI)_a}{(EI)_u + (EI)_a}\frac{\Delta\theta}{2}. \end{aligned} \tag{12}$$

The matching boundary conditions

$$V^{(n)}(0) = V^{(n)}(2\pi), \quad n = 0, 1, \ldots, 5 \tag{13}$$

are introduced to reduce the unknowns of equation (11). Applying these matching boundary conditions to equation (11), we can obtain an equation

$$\sum_{j=1}^{3} Z_j^k G_{jr} = 0, \quad k = 0, 1, \ldots, 5, \quad r = \begin{cases} 1 & (k\text{: even number}), \\ 2 & (k\text{: odd number}), \end{cases} \tag{14}$$

where

$$\begin{aligned} G_{j1} &= (a_j - 1)A_j + b_j B_j + \sum_{i=1}^{N} (c_{ij}C_{ij} + d_{ij}D_{ij}), \\ G_{j2} &= b_j A_j + (a_j - 1)B_j + \sum_{i=1}^{N} (d_{ij}C_{ij} + c_{ij}D_{ij}), \\ a_j &= \cosh(2\pi Z_j), \qquad b_j = \sinh(2\pi Z_j), \\ c_{ij} &= \cosh\{Z_j(2\pi - \theta_i)\}, \qquad d_{ij} = \sinh\{Z_j(2\pi - \theta_i)\}. \end{aligned}$$

All G_{jr} in equation (12) should be zero, because Z_j's are assumed to be different from one another. These conditions can be expressed in matrix form:

$$\begin{bmatrix} a_j - 1 & b_j \\ b_j & a_j - 1 \end{bmatrix} \begin{Bmatrix} A_j \\ B_j \end{Bmatrix} = -\begin{Bmatrix} \sum_{i=1}^{N} (c_{ij}C_{ij} + d_{ij}D_{ij}) \\ \sum_{i=1}^{N} (d_{ij}C_{ij} + c_{ij}D_{ij}) \end{Bmatrix}, \quad j = 1, 2, 3. \tag{15}$$

From the manipulation of the above equations based on reference [5], equation (11) is formulated to the equation

$$V(\theta) = -\sum_{i=1}^{N}\sum_{j=1}^{3} \frac{1}{2\sinh(\pi Z_j)}[C_{ij}\sinh\{Z_j(\theta - \theta_i + \pi)\} + D_{ij}\cosh\{Z_j(\theta - \theta_i + \pi)\}]$$

$$+ \sum_{i=1}^{N}\sum_{j=1}^{3} \mathrm{H}(\theta - \theta_i)[C_{ij}\cosh\{Z_j(\theta - \theta_i)\} + D_{ij}\sinh\{Z_j(\theta - \theta_i)\}], \tag{16}$$

where $\theta_{\mathrm{I}} < \theta_i < \theta_{\mathrm{II}}$. Assuming a Gaussian point among θ_i's as θ_k, an equation of $V(\theta_k)$ is obtained from equation (16), and if we substitute equation (12) into the equation of $V(\theta_k)$, we can formulate a relation of V, V', and V''':

$$V(\theta_k) = \sum_{i=1}^{k-1}\sum_{j=1}^{3} [\{K_{ji}F + K_{ji}\sinh(z_j\Delta_{ki})\}V(\theta_i)$$

$$+ \{I_{ji}E + I_{ji}\cosh(z_j\Delta_{ki})\}V'(\theta_i) + \{J_{ji}E + J_{ji}\cosh(z_j\Delta_{ki})\}V'''(\theta_i)]$$

$$+ \sum_{i=k}^{N}\sum_{j=1}^{3} [(K_{ji}F)V(\theta_i) + (I_{ji}E)V'(\theta_i) + (J_{ji}E)V'''(\theta_i)], \tag{17}$$

where

$$\Delta_{ki} = \theta_k - \theta_i,$$

$$E = -\frac{1}{2}\left\{\frac{\sinh(z_j\Delta_{ki})}{\tanh(\pi z_j)} + \cosh(z_j\Delta_{ki})\right\}, \quad F = -\frac{1}{2}\left\{\sinh(z_j\Delta_{ki}) + \frac{\cosh(z_j\Delta_{ki})}{\tanh(\pi z_j)}\right\},$$

$$I_{ji} = \frac{z_j}{Q_j}\lambda M^* w_i - \frac{z_j^3 + z_j}{Q_j}(EI)^* w_i, \quad J_{ji} = -\frac{z_j^3 + z_j}{Q_j}(EI)^* w_i, \quad K_{ji} = -\frac{1}{Q_j}\lambda M^* w_i.$$

From equation (17) and its derivatives, we can arrange the relations of V, V', and V''' corresponding to the kth Gaussian point ($k = 1, \ldots, N$) as

$$\sum_{i=1}^{N} [{}_0A_{ki}V(\theta_i) + {}_1A_{ki}V'(\theta_i) + {}_3A_{ki}V'''(\theta_i)] = 0,$$

$$\sum_{i=1}^{N} [{}_0B_{ki}V(\theta_i) + {}_1B_{ki}V'(\theta_i) + {}_3B_{ki}V'''(\theta_i)] = 0, \tag{18}$$

$$\sum_{i=1}^{N} [{}_0C_{ki}V(\theta_i) + {}_1C_{ki}V'(\theta_i) + {}_3C_{ki}V'''(\theta_i)] = 0,$$

TABLE 1

Geometry and material properties of the ring with widely distributed density deviation

E_u	210 GPa
ρ_u	7850 kg/m^3
ρ_a	3925 kg/m^3
R	300 mm
t_u	10 mm
h	10 mm
$\Delta\theta$	90° ($\theta_x = 45°$, $\theta_{II} = 135°$)

where coefficients of equation (18) are shown in Appendix A. Equation (18) can be represented as a simple matrix form

$$\mathbf{Mx} = \begin{bmatrix} \mathbf{M}_{11} & \mathbf{M}_{12} & \cdots & \mathbf{M}_{1N} \\ \mathbf{M}_{21} & \mathbf{M}_{22} & \cdots & \mathbf{M}_{2N} \\ \vdots & \vdots & \ddots & \vdots \\ \mathbf{M}_{N1} & \mathbf{M}_{N2} & \cdots & \mathbf{M}_{NN} \end{bmatrix} \begin{Bmatrix} \mathbf{x}_1 \\ \mathbf{x}_2 \\ \vdots \\ \mathbf{x}_N \end{Bmatrix} = 0, \tag{19}$$

where

$$\mathbf{M}_{ki} = \begin{bmatrix} {}_0A_{ki} & {}_1A_{ki} & {}_3A_{ki} \\ {}_0B_{ki} & {}_1B_{ki} & {}_3B_{ki} \\ {}_0C_{ki} & {}_1C_{ki} & {}_3C_{ki} \end{bmatrix}, \quad \mathbf{x}_i = \begin{Bmatrix} V(\theta_i) \\ V'(\theta_i) \\ V'''(\theta_i) \end{Bmatrix}.$$

The size of matrix $\mathbf{M}$ depends on the number of Gaussian points N, limiting the size because the integration using the Gauss quadrature converges very quickly with small number of Gaussian points. From the characteristic equation obtained from $\det(\mathbf{M}) = 0$, the natural frequencies of a circular ring with widely distributed deviation are obtained [7]. Once we obtain the natural frequencies, $V(\theta_i)$, $V'(\theta_i)$, and $V'''(\theta_i)$ are calculated from equation (19) and substituted into equation (12) to get C_{ij} and D_{ij} which are used in equation (16) to obtain the mode shapes.

3. VERIFICATION

The natural frequencies and mode shapes of a ring with widely distributed deviation were calculated by the method proposed in this study, and compared to the results of FE analysis and modal test. Mass and stiffness effects were verified by FE analysis, and an actual ring with a thickness deviation was built to verify the combined effect by modal test. For the integration convergence, five Gaussian points showed acceptable results, but for more accuracy, seven Gaussian points were used in this analysis.

3.1. VERIFICATION OF THE MASS AND STIFFNESS EFFECT

A circular ring shown in Table 1 was analyzed to verify the mass effect. This ring has 50% density deviation distribution over the wide range of 90°. In the FE analysis, an FE model was constructed from 720 solid elements and analyzed by a commercial FEA program

TABLE 2

Comparison of the natural frequencies of the ring with widely distributed density deviation calculated from the proposed analysis and FEA

Mode	Proposed analysis (Hz)	FEA (Hz)	Difference (%)
1-1	76·23	76·31	0·11
1-2	76·36	76·44	0·10
2-1	213·43	213·82	0·18
2-2	219·50	219·90	0·18
3-1	412·44	413·69	0·30
3-2	419·70	420·96	0·30

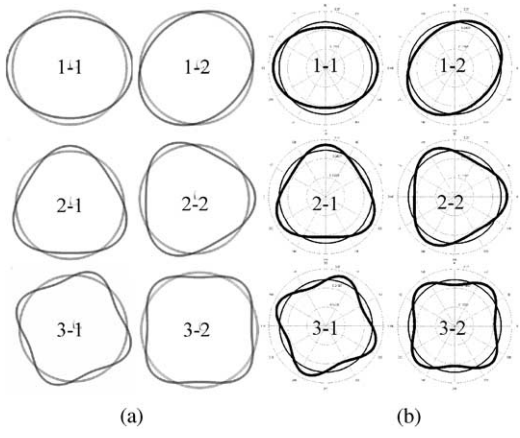

Figure 2. Mode shapes of the ring with widely distributed density deviation from (a) FEA and (b) proposed analysis.

(ANSYS). The results are compared in Table 2 and Figure 2, which show good correlation between the results of the two methods.

To verify the stiffness effect, a circular ring in Table 3 was used for the analysis. This ring has 50% stiffness deviation distribution over the wide range of 90°. The FE model of this ring also had 720 solid elements, and Young's Modulus was changed for the stiffness asymmetry. The natural frequencies and mode shapes are compared in Table 4 and Figure 3. The comparison shows that the results from the analysis proposed in this study correlate well to the results by FEA.

Figures 2 and 3 show that the middle point of the deviation region (top of the ring) is the anti-nodal point for the symmetric mode as well as the nodal point for the antisymmetric mode.

3.2. VERIFICATION OF THE COMBINED EFFECT

An actual ring that has 10% thickness deviation distribution over the range of 30° was built to verify the combined effect by modal test. Figure 1 and Table 5 show the geometry and the material property of the ring; 10% decrease of thickness is identical with 27% decrease in Young's modulus and 10% decrease in mass per unit length. An FE model of this ring was also built to compare with the other results.

TABLE 3

Geometry and material properties of the ring with widely distributed stiffness deviation

E_u	210 GPa
E_a	105 GPa
ρ_u	7850 kg/m^3
R	300 mm
t_u	10 mm
h	10 mm
$\Delta\theta$	90° ($\theta_{\mathrm{I}} = 45°$, $\theta_{\mathrm{II}} = 135°$)

TABLE 4

Comparison of the natural frequencies of the ring with widely distributed stiffness deviation calculated from the proposed analysis and FEA

Mode	Proposed analysis (Hz)	FEA (Hz)	Difference (%)
1-1	63·68	63·76	0·12
1-2	65·56	65·63	0·11
2-1	180·25	180·59	0·19
2-2	185·22	185·58	0·20
3-1	346·10	347·22	0·32
3-2	354·11	355·18	0·30

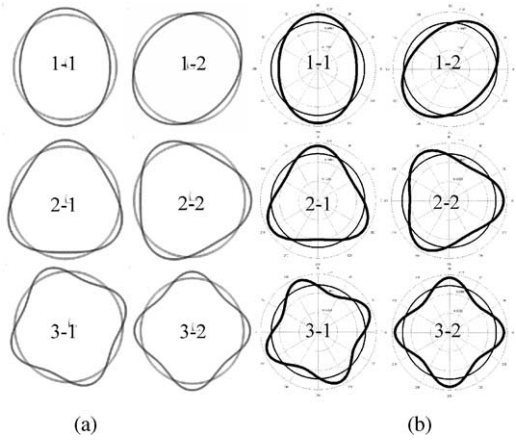

Figure 3. Mode shapes of the ring with widely distributed stiffness deviation from (a) FEA and (b) proposed analysis.

Table 6 and Figure 4 show the comparisons of the natural frequencies and the mode shapes obtained from the proposed analysis, FE analysis, and modal test. The comparisons show that the result from each method correlated well with each another. The middle point of the deviation region is also the anti-nodal point for the symmetric mode as well as the nodal point for the antisymmetric mode.

TABLE 5

Geometry and material properties of the ring with widely distributed thickness deviation

E_u	68 GPa
ρ_u	2690·8 kg/m^3
R	165 mm
h	5·8 mm
t_u	10 mm
t_a	9 mm
$\Delta\theta$	30° ($\theta_{\mathrm{I}} = 75°$, $\theta_{\mathrm{II}} = 105°$)

TABLE 6

Comparison of the natural frequencies of the ring with widely distributed thickness deviation obtained from the proposed analysis, FEA, and modal test

Mode	Proposed analysis (Hz)	FEA (Hz)	Modal test (Hz)
1-1	224·82 (0·12)	223·35 (0·53)	224·55
1-2	227·68 (0·10)	227·46 (0·00)	227·45
2-1	637·56 (0·43)	634·08 (0·11)	634·80
2-2	642·61 (0·11)	641·49 (0·06)	641·88
3-1	1224·92 (0·83)	1219·59 (0·39)	1214·86
3-2	1229·98 (0·64)	1226·95 (0·39)	1222·15

Note: The values in the parentheses are percentage errors from the modal test.

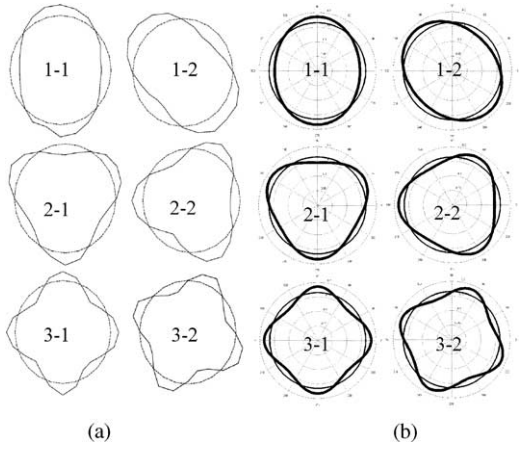

Figure 4. Mode shapes of the ring with widely distributed thickness deviation from (a) FEA and (b) proposed analysis.

4. SIMULATION OF NATURAL FREQUENCY

The natural frequencies of a ring with a distributed deviation over 30° were calculated with variations of density, stiffness, and thickness in the deviation region, using the method proposed in this study to investigate the effect of the variations on the

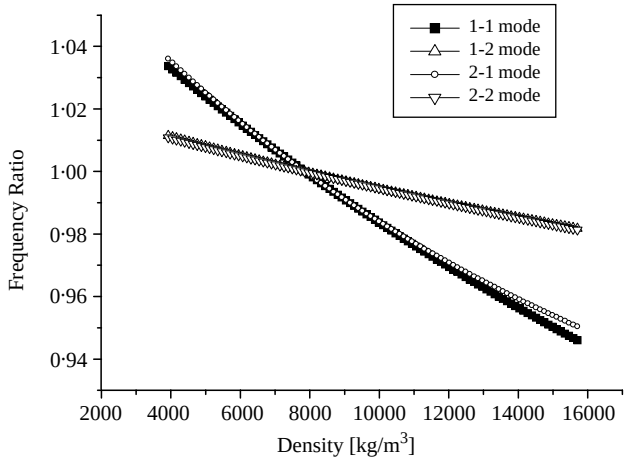

Figure 5. Natural frequency ratios with variations of the density in the deviation.

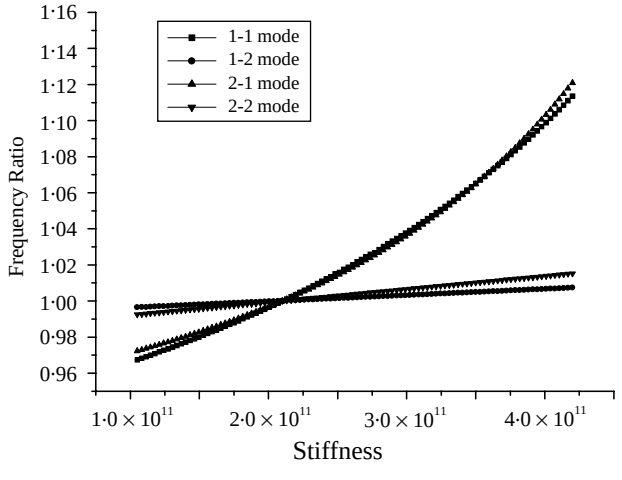

Figure 6. Natural frequency ratios with variations of the stiffness in the deviation.

natural frequencies. The simulation was conducted for the first and second natural frequencies.

4.1. NATURAL FREQUENCY CHANGE DUE TO THE MASS AND STIFFNESS VARIATION

Figure 5 shows the effect of variation in density on each natural frequency. The vertical axis is the natural frequency ratio of the deviation ring to a uniform ring. The density range, shown on the horizontal axis, is from 50 to 200% of the uniform ring's density (7850 kg/m^3). Figure 6 shows the simulation results of a ring with stiffness (Young's modulus) deviation distribution over 30°. The stiffness range, shown on the horizontal axis, is also from 50 to 200% of the uniform ring's stiffness (210 GPa).

Figures 5 and 6 reveal that the density and stiffness deviations affect the natural frequencies of the symmetric modes more than those of antisymmetric modes; specifically, the stiffness effects are greater than the mass effects on the symmetric modes. Generally, the

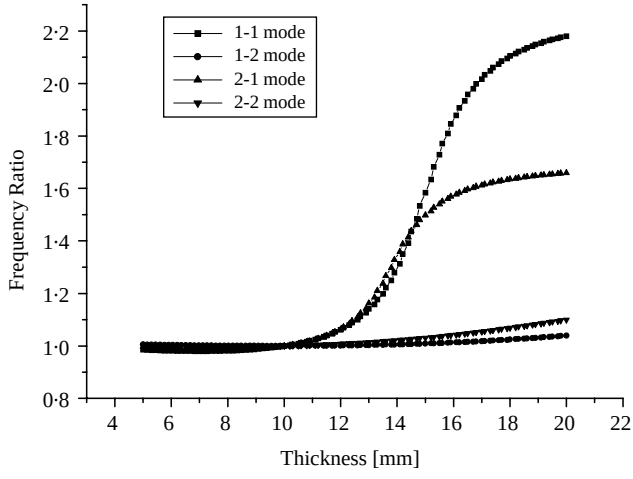

Figure 7. Natural frequency ratios with variations of the thickness in the deviation.

antisymmetric modes' natural frequencies of a ring with local stiffness deviation in a small region are same as those of a uniform ring because the local deviation is located at the nodal point that has no bending. However, the natural frequencies of a ring with a local mass deviation are slightly different from those of a uniform ring because the circumferential displacement of the nodal point is less than its radial displacement. However, Figure 6 shows the natural frequency changes of antisymmetric modes due to the deviation distribution over 30° and the bending deformation of the ring without the nodal point in this range.

4.2. NATURAL FREQUENCY CHANGE DUE TO THE THICKNESS VARIATION

Figure 7 represents the natural frequency ratio with the variation of thickness on the horizontal axis. Simulation was performed using a ring model with a density of 7850 kg/m^3 and Young's modulus of 210 GPa.The thickness range, shown on the horizontal axis, is also from 50 to 200% of the uniform ring's thickness (10 mm).

As shown in Figure 7, when the thickness in the deviation region is thinner than in the other part, the natural frequencies are not significantly changed. However, the effect of asymmetry appears significantly in the symmetric modes, when the thickness in the deviation region is thicker than that in the other part. The natural frequencies of the symmetric modes increase exponentially up to about 15 mm, and start to converge to specific natural frequencies from about 19 mm.

5. CONCLUSIONS

A new method for the eigenvalue analysis of a ring with widely distributed deviation was proposed. Laplace transform was used for the proposed analysis to find the exact solution evaluation without assuming any trial functions and finite elements, and the widely distributed deviation was effectively formulated in the theory by the Gauss–Legendre quadrature.

The natural frequencies and mode shapes of the rings with density, stiffness, and thickness deviations were calculated by the proposed method, and compared with those from FEM and modal test for the verification. Based on the verified results, more simulations were performed to investigate the effect of partial change of density, stiffness, and thickness on the natural frequencies for various cases.

ACKNOWLEDGMENT

This work was supported by the Brain Korea 21 Project.

REFERENCES

1. D. ALLAEI, W. SOEDEL and T. Y. YOUNG 1986 *Journal of Sound and Vibration* **111**, 9–27. Natural frequencies and modes of rings that deviate from perfect axisymmetry.
2. D. ALLAEI, W. SOEDEL and T. Y. YOUNG 1987 *Journal of Sound and Vibration* **121**, 547–561. Eigenvalue of rings with radial spring attachments.
3. Z. CEREP 1990 *Journal of Sound and Vibration* **143**, 461–471. In-plane vibrations of circular rings on tensionless foundation.
4. R. E. ROSSI 1989 *Journal of Sound and Vibration* **135**, 443–452. In-plane vibration of circular rings of non-uniform cross-section with account taken of shear and rotatory inertia effects.
5. J. S. HONG and J. M. LEE 1994 *Transactions of the American Society of Mechanical Engineers, Journal of Applied Mechanics* **61**, 317–322. Vibration of circular ring with local deviation.
6. R. H. GUTIERREZ and P. A. A. LAURA 1995 *Journal of Sound and Vibration* **185**, 507–513. Vibration of non-uniform rings studied by means of the differential quadrature method.
7. R. N. WAKE, J. S. BURDESS and J. T. EVANS 1998 *Journal of Sound and Vibration* **214**, 761–770. Changes in the natural frequencies of repeated mode pairs induced by cracks in a vibrating ring.
8. R. S. HWANG, C. H. J. FOX and S. MCWILLIAM 1999 *Journal of Sound and Vibration* **220**, 497–516. The in-plane vibration of thin rings with in-plane profile variations. Part I: general background and theoretical formulation.
9. R. S. HWANG, C. H. J. FOX and S. MCWILLIAM 1999 *Journal of Sound and Vibration* **220**, 517–539. The in-plane vibration of thin rings with in-plane profile variations. Part II: application to nominally circular rings.
10. J. CHUNG and J. M. LEE 1999 *Journal of Sound and Vibration* **219**, 35–50. Vibration analysis of a nearly axisymmetric shell structure using a new finite ring element.
11. S. H. KIM, W. SOEDEL and J. M. LEE 1994 *Journal of Sound and Vibration* **173**, 517–536. Analysis of the beating response of bell type structures.
12. A. E. H. LOVE 1944 *A Treatise on the Mathematical Theory of Elasticity*. New York: Dover, fourth edition.
13. W. SOEDEL 1993 *Vibration of Shells and Plates*. New York: Marcel Dekker, second edition.
14. M. R. SPIEGEL 1983 *Theory and Problems of Advanced Mathematics for Engineers and Scientists*. New York: McGraw-Hill.

APPENDIX A

The coefficients of equation (18)

$(1 \leqslant i \leqslant k-1)$

$$
{}_0A_{ki} = \sum_{j=1}^{3} K(F+S), \quad {}_1A_{ki} = \sum_{j=1}^{3} I(E+C), \quad {}_3A_{ki} = \sum_{j=1}^{3} J(E+C),
$$

$$
{}_0B_{ki} = \sum_{j=1}^{3} Z_j K(E+C), \quad {}_1B_{ki} = \sum_{j=1}^{3} Z_j I(F+S), \quad {}_3B_{ki} = \sum_{j=1}^{3} Z_j J(F+S),
$$

$$
{}_0C_{ki} = \sum_{j=1}^{3} Z_j^3 K(E+C), \quad {}_1C_{ki} = \sum_{j=1}^{3} Z_j^3 I(F+S), \quad {}_3C_{ki} = \sum_{j=1}^{3} Z_j^3 J(F+S).
$$

$(i = k)$

$$
{}_0A_{ki} = \sum_{j=1}^{3} (FK) - 1, \qquad {}_1A_{ki} = \sum_{j=1}^{3} I(E + C), \qquad {}_3A_{ki} = \sum_{j=1}^{3} J(E + C),
$$

$$
{}_0B_{ki} = \sum_{j=1}^{3} Z_j K(E + C), \qquad {}_1B_{ki} = \sum_{j=1}^{3} (Z_j FI) - 1, \qquad {}_3B_{ki} = \sum_{j=1}^{3} (Z_j FJ),
$$

$$
{}_0C_{ki} = \sum_{j=1}^{3} Z_j^3 K(E + C), \qquad {}_1C_{ki} = \sum_{j=1}^{3} (Z_j^3 FI), \qquad {}_3C_{ki} = \sum_{j=1}^{3} (Z_j^3 FJ) - 1.
$$

$(k + 1 \leqslant i \leqslant n)$

$$
{}_0A_{ki} = \sum_{j=1}^{3} (FK), \qquad {}_1A_{ki} = \sum_{j=1}^{3} (EI), \qquad {}_3A_{ki} = \sum_{j=1}^{3} (EJ),
$$

$$
{}_0B_{ki} = \sum_{j=1}^{3} (Z_j EK), \qquad {}_1B_{ki} = \sum_{j=1}^{3} (Z_j FI), \qquad {}_3B_{ki} = \sum_{j=1}^{3} (Z_j FJ),
$$

$$
{}_0C_{ki} = \sum_{j=1}^{3} (Z_j^3 EK), \qquad {}_1C_{ki} = \sum_{j=1}^{3} (Z_j^3 FI), \qquad {}_3C_{ki} = \sum_{j=1}^{3} (Z_j^3 FJ),
$$

where

$$
I = I_{ji}, J = J_{ji}, K = K_{ji},
$$

$$
S = \sinh(\Delta_{ki} Z_j), C = \cosh(\Delta_{ki} Z_j).
$$

APPENDIX B: NOMENCLATURE

w_i	weighting coefficient for Gaussian quadrature
E	Young's modulus
M^*	equivalent mass of the partial deviation
$(EI)^*$	equivalent bending stiffness of the partial deviation
H_i	step function of $\mathrm{H}(\theta - \theta_i)$
m_a	added mass per unit length
R	radius of the neutral surface of the circular ring
$V(\theta)$	circumferential displacement of the circular ring
δ_i	delta function of $\delta(\theta - \theta_i)$
θ_{I}	starting position of the partial deviation
θ_{II}	ending position of the partial deviation
$\Delta\theta$	angle of the partial deviation